

EPJ B

Condensed Matter
and Complex Systems

EPJ.org

your physics journal

Eur. Phys. J. B (2015) 88: 53

DOI: [10.1140/epjb/e2015-50659-7](https://doi.org/10.1140/epjb/e2015-50659-7)

Systems confined by pusher multiplicative noises

Sergio E. Mangioni

 **edp sciences**



 **Springer**

Systems confined by pusher multiplicative noises

Sergio E. Mangioni^a

IFIMAR (Universidad Nacional de Mar del Plata and CONICET), Dean Funes 3350, B7602AYL Mar del Plata, Argentina

Received 25 September 2014 / Received in final form 4 November 2014

Published online 9 March 2015 – © EDP Sciences, Società Italiana di Fisica, Springer-Verlag 2015

Abstract. We frequently employ the intuitive concept that a multiplicative noise can expel a system towards the field values for which intensity is negligible. This process applies even when such noise effects are opposed to the deterministic forces. In addition, it has been stated that a system may be confined by such noise within a field values region, distant from the stationary homogeneous solutions. In order to promote or explain noise-induced ordering phase transitions, the gradient of the multiplicative factor of noise is employed as if it were a force. However, there has not been a thorough study of this concept in the literature to date. In this paper, we conduct such a study.

1 Introduction

Currently, there is a great deal of activity and interest generated by the subject of the constructive effect of noise on the dynamics of complex systems [1–5]. Among numerous examples, noise-induced ordering phase transitions (transitions between true extended phases) are of fundamental importance. These can be divided into two classes. The first case to be studied, was explained in terms of a noise-induced short-time instability in the local dynamics, collectively sustained in a long time limit by spatial coupling [6–10]. These ordering phase transitions are characterized by being reentrant with the noise intensity. Initially it was erroneously assumed that the zero-dimensional models exhibiting noise-induced transitions [11], were not able to show any interesting behavior when coupled. However, Ibañez and co-workers [12–14] have found a second class of noise-induced phase transitions showing that it is not so. They introduced an illustrative generic model that describes relaxational dynamics in a free-energy functional, with kinetic coefficients depending on the field. This model is subject to a Gaussian white noise whose multiplicative factor, in order to fulfill the fluctuation-dissipation relation, is the square root of this coefficient. Several differences can be pointed out between both cases: (a) in the 2nd case, at short times, the disordered phase is stable; (b) through the calculation of the exact stationary probability distribution, which is possible in the 2nd case, it can be seen that the disordered phase is destabilized at long times, giving rise to more ordered solutions; (c) for the 2nd case, a transition (although not a phase transition) also happens in zero-dimensional cases; (d) the transitions, that for the 1st case are reentrant (a case was recently reported [15]), usually are not in the

2nd, but rather they become more ordered as the noise intensity increases.

Both physical contexts have been used to study pattern formation [4]. For the purposes of this study, it is the second class of noise-induced ordering phase transitions which matters¹. In this regard, over time, some researchers had a hunch that a multiplicative noise may expel the system from the field values region in which the noise is more intense towards another in which the effects of noise are not significant. Furthermore, the following concept was introduced: a field increased noise multiplicative factor can push the system towards regions where the noise intensity is negligible, confining it to this last region in order to enable a mechanism of pattern creation [19–21]. In fact, the possibility to force a pinning mechanism using this strategy has been recently proposed and verified [22].

Even though the report of the results based on this hunch has been positive, there is not a thorough study on this subject to date. Therefore, we decided to conduct this study using a bi-stable and zero-dimensional model affected by a white noise, whose multiplicative factor decreases exponentially with the field, from the edge of the region of confinement towards its inside.

First, we describe the model, then we show the results for a reasonable range of parameters, and finally, we propose our conclusions.

¹ Some illustrative works have been reported [16–18]. They exhibit an equation like the one in [12–14], taking a similar local potential to build the free energy, but replacing the traditional diffusive term (Fick's law) by the Swift-Hohenberg one. They also consider an appropriate form for the kinetic coefficient for each potential. In this way the system is expelled from the disordered phase due to the multiplicative noise, and a competition is introduced between two length scales by means of the Swift-Hohenberg operator, which generates a morphological instability.

^a e-mail: smangio@mdp.edu.ar

2 Model

Let us consider the following reaction-diffusion equation:

$$\partial_t u = Q(u) + \partial_x [D(u) \partial_x u,]. \quad (1)$$

$Q(u)$ is the deterministic force and $D(u)$ the field-dependent diffusion coefficient. Given any field-dependent relaxation coefficient $\Gamma(u)$, a dynamical with relaxational flow can be written as:

$$\partial_t u = -\Gamma(u) \frac{\delta \mathcal{F}[u(x)]}{\delta u(x)}, \quad (2)$$

indicating that the dynamics is relaxational in some free-energy functional $\mathcal{F}[u(x)]$ with a field-dependent kinetic coefficient $\Gamma(u)$. By adding to this dynamics a Gaussian white noise with zero mean, correlation

$$\langle \eta(x, t) \eta(x', t') \rangle = 2\bar{\lambda}^2 \delta(x - x') \delta(t - t')$$

and multiplicative factor $\Gamma^{1/2}(u)$ (which moreover fulfills the fluctuation-dissipation theorem), we obtain

$$\partial_t u = -\Gamma(u) \frac{\delta \mathcal{F}[u(x)]}{\delta u(x)} + \Gamma^{1/2}(u) \eta(x, t). \quad (3)$$

Then, we can calculate the average effect of this noise without even knowing the functional form of $\mathcal{F}[u(x)]$ [12,13,23]. The corresponding average dynamics can be described by an effective functional [19–21,23]

$$\mathcal{F}_\beta[u(x)] = \mathcal{F}[u(x)] + \beta \int_{-L}^L dx \ln \Gamma(u),$$

which is the previous functional modified by the effect of noise, being the control parameter β proportional to the noise intensity (if the $[-L, L]$ interval is discretized with step δx , then $\beta = \frac{\delta x}{2} \bar{\lambda}^2$ [12,13,23]). Replacing $\mathcal{F}_\lambda[\phi(x)]$ by $\mathcal{F}[\phi(x)]$ in equation (2) and recovering the form of equation (1), we obtain

$$Q_\lambda(u) = Q(u) - \beta \frac{d\Gamma}{du}.$$

The above relationship is even valid for zero-dimensional case and it has been used to substantiate that a system can be pushed by the multiplicative noise toward the field values for which $Q_\lambda(u) = 0$ [19–21]. Also, due to this effect, it is possible to confine the system within a region in which the noise is imperceptible.

As mentioned in the introduction, we limit our thorough study to a zero-dimensional model and choose the following normal form as a deterministic force:

$$Q(u) = u(1 - u^2)$$

(two $-u_{hs} = \pm 1$ – stable and $-u_{hs} = 0$ – one unstable solutions). In this way, the stochastic equation which describes the dynamics of the system is written as:

$$\partial_t u = Q(u) + \Gamma^{1/2}(u) \eta(t), \quad (4)$$

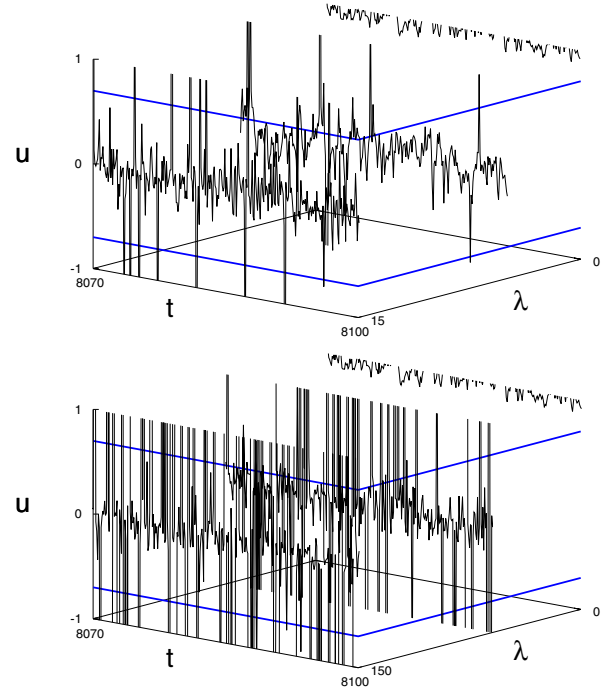


Fig. 1. Evolution of the field $u(t)$ for $b = 5$. (Top) $\lambda = 0.1, 5, 15$. (Bottom) $\lambda = 0.1, 60, 150$. The lines with $u = \pm 0.7$ indicate the boundaries of the confinement region ($u_l = \pm 0.7$).

being the correlation

$$\langle \eta(t) \eta(t') \rangle = 2\bar{\lambda}^2 \delta(t - t').$$

We decided to confine the system to a region between the two stable solutions: $u \in (-u_l, +u_l)$ with $u_l < 1$. We proposed the following multiplicative factor of noise to achieve our goal:

$$\begin{aligned} \Gamma_u &:= \exp[2b(|u| - u_l)] \text{ if } |u| < u_l, \\ \Gamma_u &:= 1 \text{ if } |u| > u_l. \end{aligned}$$

Thus, the effect of the noise decreases exponentially within the region of confinement and it is maintained at its maximum intensity level in the forbidden region.

Considering the selected non-linearity, a symmetry between the negative and positive values of u is expected.

3 Results

In order to observe the effectiveness of the confinement, we solved the stochastic equation numerically (4) using a Heun scheme [24,25] with a time step $\Delta t = 10^{-5}$. Here, we only display cases with $u_l = 0.7$ (confinement region localized between $u = 0.7$ and $u = -0.7$) and initiated (zero time) from any positive value of u between 0 and 1.5. Thus, we also observed other cases initiated from u negative and we obtained the same statistical results, but with a changed sign.

Figure 1 shows a window ($\Delta t_w = 30$) of the evolution of field u for $b = 5$ and different noise intensities.

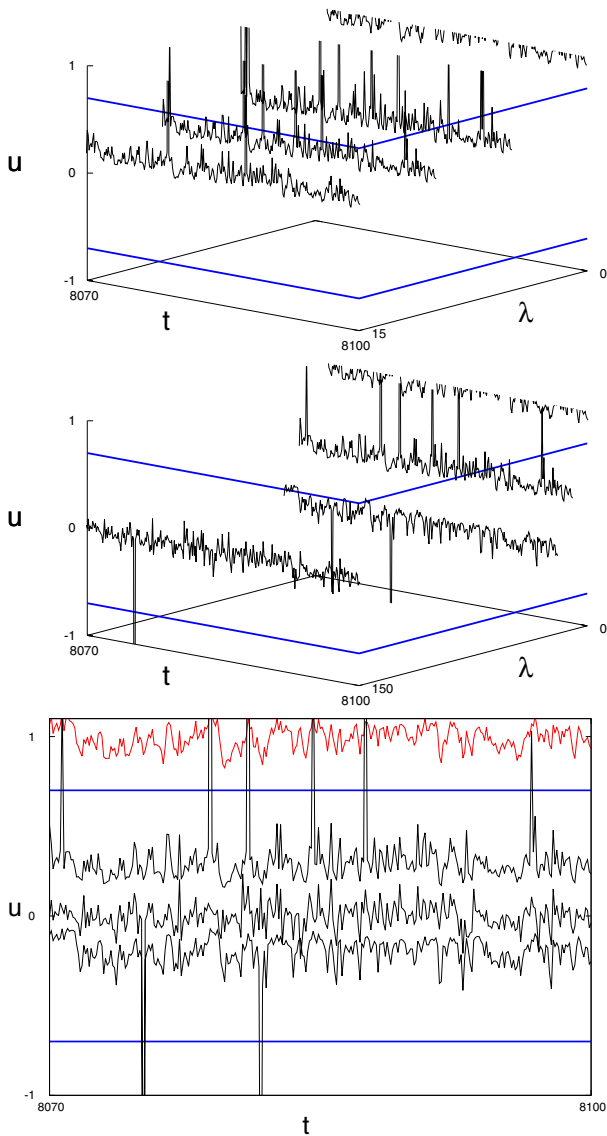


Fig. 2. Evolution of the field $u(t)$ for $b = 10$. (Top) $\lambda = 0.1, 5, 10, 15$. (Center) $\lambda = 0.1, 10, 20, 150$. (Bottom) View in 2D idem above. The lines with $u = \text{constant}$ indicate the boundaries of the confinement region ($u_l = \pm 7$).

The lines with $u = \text{constant}$ indicate the boundaries of the confinement region. We noted that the evolution of $u(t)$ was calculated up to 10^5 .

The curves show that for a high enough λ , the confinement is quite effective, but it declines for an even higher λ . This suggests the existence of an optimal value for the noise intensity ($\lambda \sim 5$). We can see that the confined solution (thus named when u is within the confinement region) is pushed toward the unstable solution ($u = 0$) fluctuating around it. The confined solution's fluctuations are quite important and its size tends to decrease smoothly with λ .

Then, we increased b . Figure 2 shows the result for $b = 10$. It is clear that the confinement becomes much more effective and improves with the increase of λ (an optimal value is not detected). In this case, u (within the

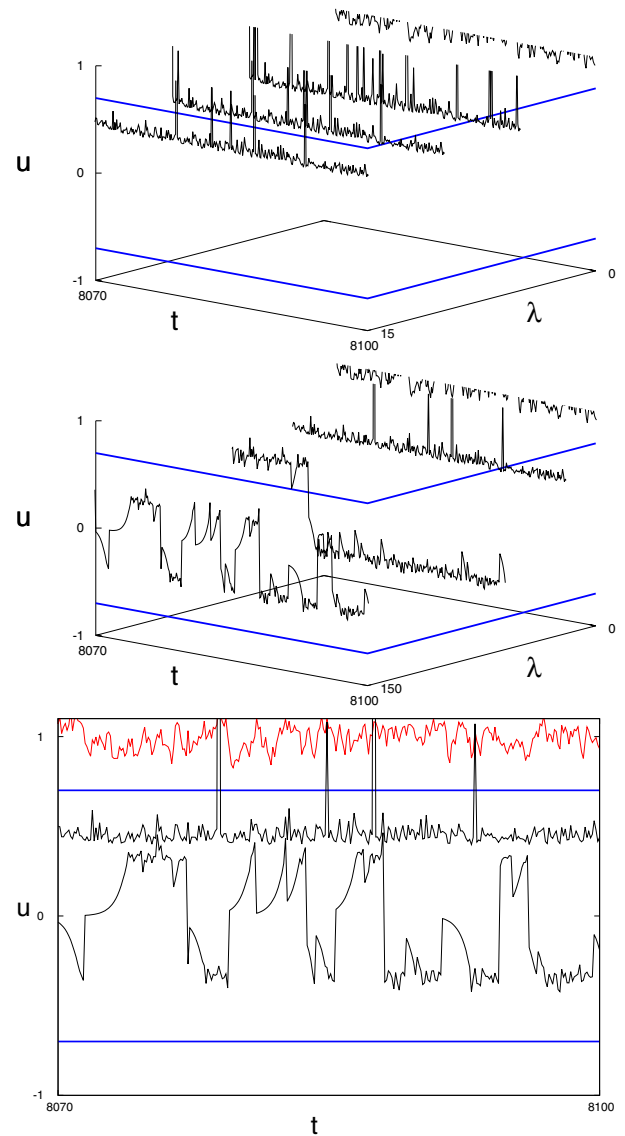


Fig. 3. Evolution of the field $u(t)$ for $b = 20$. (Top) $\lambda = 0.1, 5, 10, 15$. (Center) $\lambda = 0.1, 20, 60, 150$. (Bottom) View in 2D idem above except $\lambda = 0.1, 20, 60$. The lines with $u = \text{constant}$ indicate the boundaries of the confinement region ($u_l = \pm 7$).

region of confinement) fluctuates around a positive average value (called U) that decreases toward zero, with the increase of λ . We explain that when the value of u in zero time is negative, the curves are as the mirror image (approximately the same absolute values of u but on the negative side) of the previously shown curves (Fig. 2). At the same time, the fluctuations' size is much lower than that observed in the previous case. There were no significant changes detected when varying the noise intensity.

Figure 3 shows the result for $b = 20$. It can be observed that from a certain λ value onwards, the curves display transitions between the two possible solutions localized within the region of confinement. Moreover, the effectiveness of the confinement does not seem to vary with the

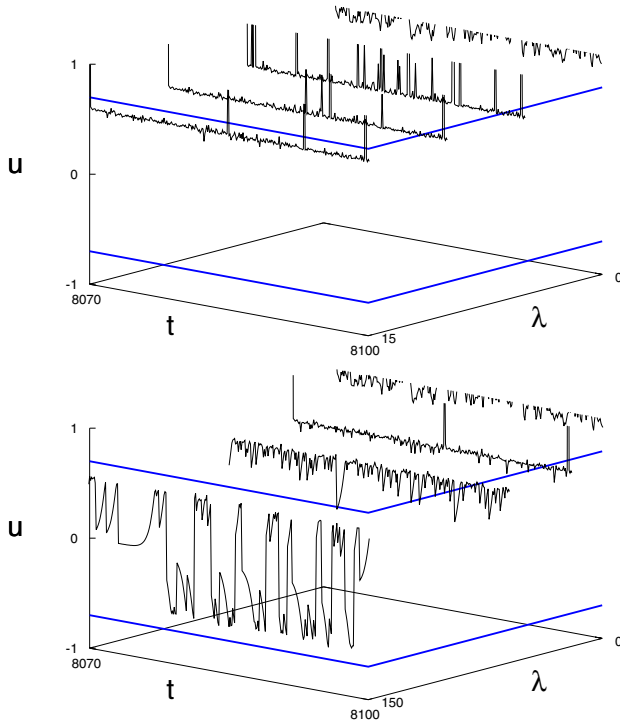


Fig. 4. Evolution of the field $u(t)$ for $b = 50$. (Top) $\lambda = 0.1, 5, 10, 15$. (Bottom) $\lambda = 0.1, 20, 60, 150$. The lines with $u = \pm 0.7$ indicate the boundaries of the confinement region ($u_l = \pm 0.7$).

increase of b , although we observed a decrease in the fluctuations' size and an increase in U . As in the previous case, if we initiate the system with a negative value of u , the corresponding curves are the mirror image of the ones displayed here.

Figure 4 shows the result for $b = 50$. Here, the most noticeable change is that transitions occur for higher λ . It can also be noted that the fluctuations' size decreases (only for $\lambda \leq 15$), whereas U increases slightly and the number of transitions is larger.

For $b = 100$ we only noticed an increase in the size of the fluctuations for higher λ and a decrease for lower λ (we did not consider it necessary to show the corresponding curves).

We recall that, although the stochastic process was initiated from different field values (outside and inside the confinement region), we did not observe differences in the results, except in those results which correspond to two possible symmetric solutions. In the cases where transitions were unlikely to occur, and as long as the process was initiated from a negative/positive field, the system was confined in the negative-positive side, fulfilling the expected symmetry for medium values of the parameters (same probability of overcoming the limits $\pm u_l$ – which we called “limit walls” –, same $|U|$ and same fluctuations' size). The same average number of transitions was also verified in cases in which transitions are likely to occur.

On the other hand, we also calculated the stationary probability density $P_{st}(u)$. To do this, we used an efficient

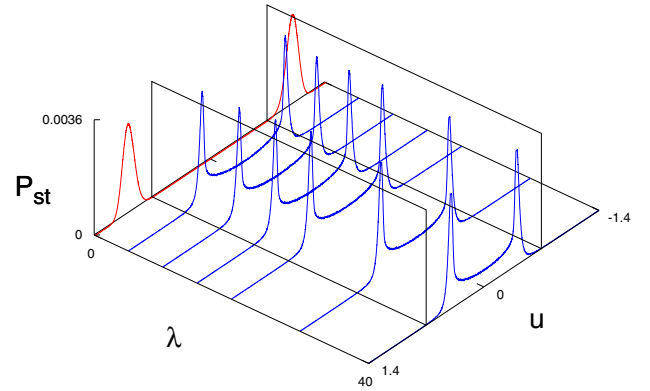


Fig. 5. Stationary probability (P_{st}) vs. u and λ . For the first curve $b = 0$ ($\lambda = \sqrt{0.2}$) and the rest $b = 20$. The lines with $u = \pm 0.7$ indicate the boundaries of the confinement region ($u_l = \pm 0.7$).

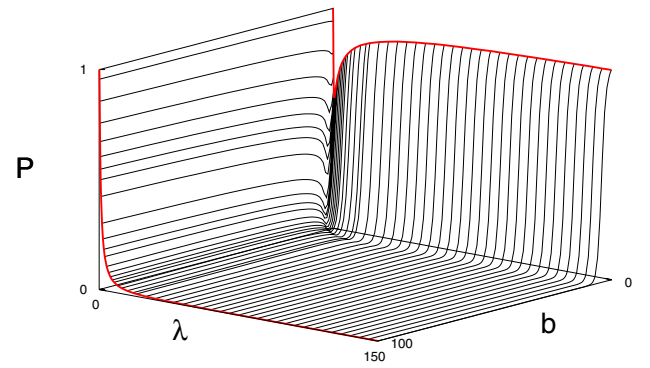


Fig. 6. Probability (P) that the field exceeds limit walls ($u_l = \pm 0.7$) vs. b and λ .

algorithm reported recently [26]. Figure 5 shows P_{st} vs. u for $b = 0$ (additive noise) – $\lambda = \sqrt{0.2}$ and $b = 20$ – $\lambda = 5, 15, 20, 30, 40$. It can be observed that the peaks of probability are displaced from the region prohibited ($b = 0$ – additive noise – and $\lambda = \sqrt{0.2}$) to the confinement region. We noted that the fact that a multiplicative noise pushes the stationary solutions in order to confine them within a given region can be interpreted as a sort of noise-induced transition.

To organize all these observations, we established the probability (P) that the field exceeded the limit walls ($\pm u_l$), basically as the normalized ratio between the times when it overcame the limit walls and those times when it didn't. Then, we calculated P for different values of λ and b , as well as for U and its corresponding standard deviation (σ).

Figures 6 and 7 show P vs. λ and b . It can be observed that whenever λ and b are large enough, the confinement is effective. Furthermore, the probability monotonously decays for large λ and b , although the curves $P(b)$ show a minimum which is much more pronounced for small enough λ (almost imperceptible for large λ). On the other hand, the curves $P(\lambda)$ also show a minimum, but only for small enough b .

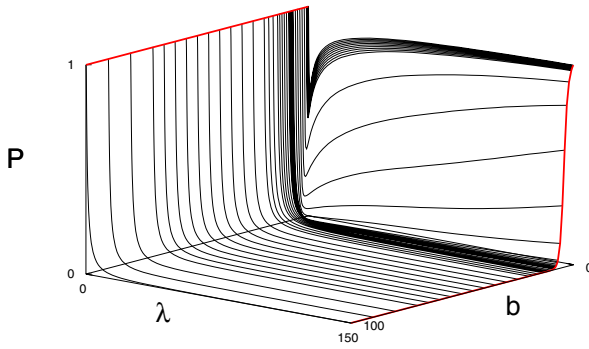


Fig. 7. Probability (P) that the field exceeds limit walls ($u_l = \pm 0.7$) vs. b and λ .

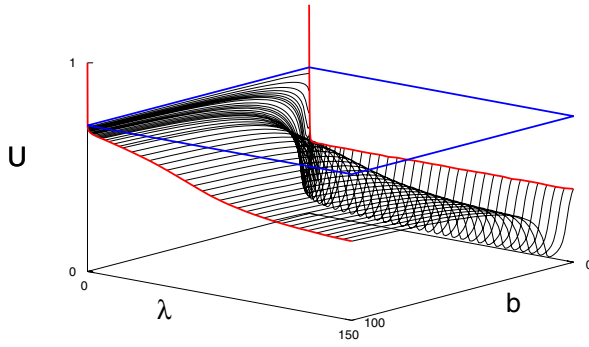


Fig. 8. $U = \langle u(t) \rangle$ vs. b and λ ($u_l = \pm 0.7$).

Figure 8 shows U vs. λ and b . Here, we only display the positive solution, since the negative is a specular reflection of the positive.

While the existence of a minimum value of U for a given low b is clear, we can see that U decreases continuously with λ . This occurs much more rapidly before and within the basin of the minimum than out of it. In fact, U quickly adopts values which are close to zero around the minimum. At the same time, U varies very little with b beyond the basin.

Figure 9 shows a standard deviation (σ) of U vs. λ and b . Although σ is quite low for low λ (wherever b is large enough), a commitment exists in relation to the effectiveness of the confinement, since P decreases with λ . It can also be observed that while there is a minimum σ for a low enough b , the confinement is not effective within these values. On the other hand, within the region in which the confinement is really effective (higher λ and b), σ reaches an ($\sigma \approx 0.03$) approximately constant value.

We noted that these curves provide a decision criterion for prioritizing some aspects over others, thus choosing between enhancing the effectiveness of confinement, a determined U value, and/or the fluctuations' size.

The curves in Figures 3 and 4 show that the frequency of transitions between the two possible solutions depends on the values of λ and b . We calculated the average life time (τ) for each solution in order to observe this phenomenon in detail. First, we chose a frequency sample (one sample every 10 000 time steps, in such a way that these are independent) and then counted the number of

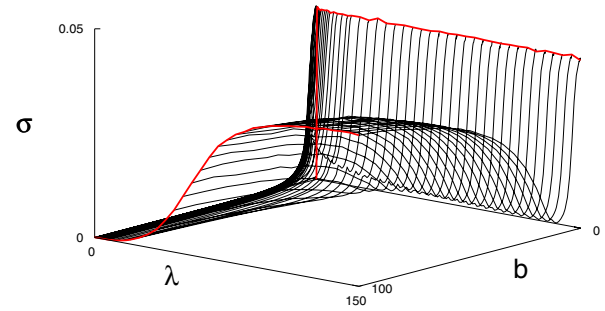


Fig. 9. Standard deviation (σ) vs. b and λ ($u_l = \pm 0.7$).

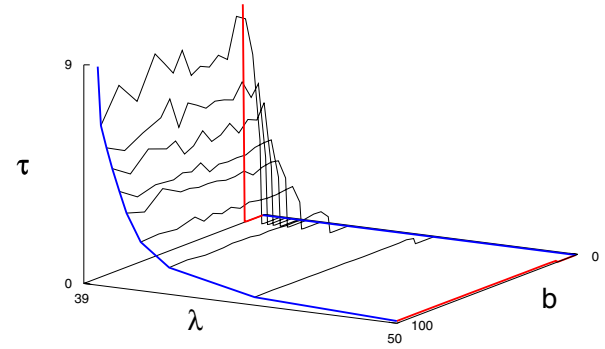


Fig. 10. Confined solution average life time (τ) vs. b and λ ($u_l = \pm 0.7$).

transitions on 3.24×10^{10} time steps. Even though we only considered samples in which the system was confined in order to calculate the norm, for cases of interest (region of parameter values where the confinement is very effective), this does not differ significantly from the total samples. Finally, we defined τ for a given solution as the quotient between the number of samples in which the system was at that solution and the number of transitions towards the other solutions.

Figure 10 shows τ vs. λ and b . The observed step with increasing b is surprising. It points out the existence of a critical b (b_c) value that separates two types of behavior (an order transition):

- for $b < b_c$, τ is very low and does not vary significantly; either with λ , or in b ;
- for $b > b_c$, τ is significantly higher and it decreases very rapidly with λ although neither varies with b .

The value of b_c varies very little with λ ($b_c = 10 - \lambda = 15$, $b_c = 12 - \lambda = 60$). We clarify that the figure only shows results for λ between 39 and 50, but we did the calculations for a larger range [0.1–150]. In particular, for low enough λ , we did not observed transitions between the two confined solutions (calculation time: 3.24×10^{10} steps).

We questioned the reason for this order transition, and we found the answer by observing the curves in Figure 8. These show that U , as a function of b , presents a pronounced minimum around $b = 10$ – 12 , just inside values that include critical b . Within the basin, the U values are close to zero, and therefore the two confined solutions are very close to each other. This favors the transitions between them (given that $Q_\lambda(u)$ represents our non-linearity

of reference; it is expected that the corresponding potential barrier increases with U). Beyond the basin, U moves abruptly and sufficiently away from zero and, therefore, the transitions between solutions are less likely to occur. This explains the sudden change of τ when $b = b_c$ (step). Consistent with this explanation, for $b > b_c$, as λ decreases, U moves away from zero and, thus, lifetime average τ grows. Moreover, for $b < b_c$, U changes very little with λ , therefore, the same happens with τ .

4 Summary and conclusions

The results shown here serve as a basis for those hypotheses which suggest that the stationary solutions corresponding to a given system can be pushed by a multiplicative noise towards a given or selected field values region that describes the system. Thus, it is possible to confine the system to that region. For this study, we chose a zero-dimensional model that includes a bi-stable normal form and a white noise with a decreasing exponentially multiplicative factor from the edge of the region of confinement towards its interior, characterized by a parameter (b) that multiplies the exponent. Through appropriate numerical simulations, we have shown that the system can be effectively confined in the chosen region. In this regard, the behavior of the stationary probability density affected by such noise (see Fig. 5) is illustrative. The relevant parameters for this proposal are the noise intensity (λ) and b .

In order to check the characteristics of the confinement, we first defined four parameters: (1) the probability (P) of escaping the region of confinement; (2) the average field value (U) in the region of confinement; (3) the standard deviation (σ) of U and (4) the life time average (τ) of both confined solutions – two solutions because of the bi-stability in the normal form. We observed that whenever b and λ are large enough, the confinement is effective. When the confinement is within the region of effectiveness, it presents different characteristics depending on the values of b and λ . Both U and the size of its fluctuations (σ) can take different values and there may also be regions where the transitions among the confined solutions are either very likely or likely to occur, and some where they are unlikely to occur. Each of these features can be selected by choosing the appropriate value for the intensity of noise and b .

A fact that initially surprised us was that the profile of $\tau(b)$ presents a step that indicates an order transition. After carefully observing the previous results – in particular the surface of $U(b, \lambda)$ – we were able to find a reasonable explanation for this step. We understood that this phenomenon is related to a pronounced minimum around critical b (b_c) exhibited by the curves of $U(b)$ for constant λ .

We believe that these results are generally applicable, and support a premise that has been successfully used on several occasions. Eventhough it is difficult to implement an experimental design of a given multiplicative factor of

noise², some can occur naturally. In such cases, their effect can be interpreted within the framework of our results.

I acknowledge financial support from CONICET, Argentina; and UNMdP, Argentina, EXA603/12.

References

1. L. Gammaitoni, P. Hänggi, P. Jung, F. Marchesoni, *Rev. Mod. Phys.* **70**, 223 (1998)
2. J. García-Ojalvo, J.M. Sancho, *Noise in Spatially Extended System* (Springer-Verlag, New York, 1999)
3. P. Reimann, *Phys. Rep.* **361**, 57 (2013)
4. F. Sagués, J.M. Sancho, J. García-Ojalvo, *Rev. Mod. Phys.* **79**, 829 (2007)
5. R. Toral, C.J. Tessone, J. Viana Lopez, *Eur. Phys. J. Special Topics* **143**, 59 (2007)
6. C. Van den Broeck, J.M.R. Parrondo, R. Toral, *Phys. Rev. Lett.* **73**, 3395 (1994)
7. C. Van den Broeck, J.M.R. Parrondo, R. Toral, R. Kawai, *Phys. Rev. E* **55**, 4084 (1997)
8. S. Mangioni, R. Deza, H.S. Wio, R. Toral, *Phys. Rev. Lett.* **79**, 2389 (1997)
9. S. Mangioni, R. Deza, R. Toral, H.S. Wio, *Phys. Rev. E* **61**, 223 (2000)
10. S.E. Mangioni, R. Deza, H.S. Wio, *Phys. Rev. E* **63**, 041115 (2001)
11. W. Horsthemke, R. Lefever, *Noise Induced Transitions* (Springer, Berlin, 1984)
12. M. Ibañes, J. García-Ojalvo, R. Toral, J.M. Sancho, *Phys. Rev. Lett.* **87**, 020601 (2001)
13. O. Carrillo, M. Ibañes, J. García-Ojalvo, J. Casademunt, J.M. Sancho, *Phys. Rev. E* **67**, 046110 (2003)
14. J. Buceta, K. Lindenberg, *Phys. Rev. E* **69**, 011102 (2004)
15. H.S. Wio, in *22nd International Conference on Noise and Fluctuations, 2013*, DOI 10.1109/ICNF.2013.6578909
16. J. Buceta, M. Ibañes, J.M. Sancho, K. Lindenberg, *Phys. Rev. E* **67**, 021113 (2003)
17. K. Wood, J. Buceta, K. Lindenberg, *Phys. Rev. E* **73**, 022101 (2006)
18. B. von Haeften, G. Izús, S. Mangioni, A.D. Sánchez, H.S. Wio, *Phys. Rev. E* **69**, 021107 (2004)
19. S.E. Mangioni, *Physica A* **389**, 1799 (2010)
20. S.E. Mangioni, R. Deza, *Phys. Rev. E* **82**, 042101 (2010)
21. S.E. Mangioni, R.R. Deza, *Physica A* **391**, 4191 (2012)
22. S.E. Mangioni, R.R. Deza, submitted
23. S.E. Mangioni, H.S. Wio, *Phys. Rev. E* **71**, 056203 (2005)
24. P. Kloeden, E. Platen, in *Numerical Solution of Stochastic Differential Equations* (Springer, Berlin, 2011), Vol. 23
25. M. San Miguel, R. Toral, in *Instabilities and Nonequilibrium Structures VI*, edited by E. Tirapegui, J. Martinez, R. Tiemann (Kluwer Academic, Dordrecht, 2000), p. 35130
26. J.A. Kromer, L. Schimansky-Geier, R. Toral, *Phys. Rev. E* **87**, 063311 (2013)

² In a photosensitive reaction, this could be done (at least down to the pixel scale) by means of computer-controlled masks, implemented with the screen of a discarded but running laptop.